

# Molecular-Weight Dependence of the Optical Rotation of Poly((*R*)-2-deuterio-*n*-hexyl isocyanate)

Hong Gu, Yo Nakamura, Takahiro Sato, and Akio Teramoto\*

Department of Macromolecular Science, Osaka University, Toyonaka, Osaka, 560 Japan

Mark M. Green,\* Christopher Andreola,<sup>†</sup> and Norman C. Peterson

Department of Chemistry and Polymer Research Institute, Polytechnic University, Six Metrotech Center, Brooklyn, New York 11201

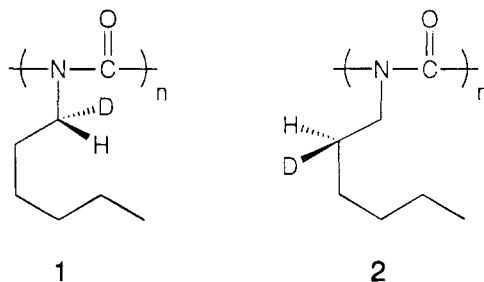
Shneior Lifson\*

Department of Chemical Physics, Weizmann Institute of Science, Rehovot 76100, Israel

Received August 2, 1994; Revised Manuscript Received October 31, 1994\*

**ABSTRACT:** The extraordinarily large optical rotations  $[\alpha]$  of poly((*R*)-2-deuterio-*n*-hexyl isocyanate) were investigated with a particular emphasis on the chain length dependence of  $[\alpha]$ . Data for  $[\alpha]$  in hexane, 1-chlorobutane, and dichloromethane were obtained as functions of temperature and degree of polymerization  $N$  and analyzed by a statistical mechanical theory developed recently (Lifson, S.; Andreola, C.; Peterson, N. C.; Green, M. M. *J. Am. Chem. Soc.* **1989**, *111*, 8850). The theory is based on a model whereby a polymer chain consists of an alternate sequence of *M* helix (left-handed) and *P* helix (right-handed), interrupted by helix reversal points, and  $[\alpha]$  originates from the excess presence of the *P* helix over the *M* helix due to the chiral substitution of a deuterium atom on the side chain. Detailed analysis of  $[\alpha]$  vs  $N$  data substantiated the validity of the theory and allowed a separate estimate of enthalpic and entropic contributions to the isotope effect, revealing that the *P* helix dwells in a slightly narrow but deep energy well in the conformational space compared with the *M* helix. In hexane at 25 °C, this isotope effect favors the *P* helix over the *M* helix by 0.74 cal mol<sup>-1</sup> on a monomer unit basis, implying that the *P* helix would exist in excess of the *M* helix only by 0.12%. However, for a long chain with  $N = 2000$ , this minute excess is amplified by the cooperative mechanism to 67:33 in  $[\alpha]$ , whereas the helix reversal costs 3900 cal mol<sup>-1</sup> and appears only once in 762 units on the average.

As reported in previous communications,<sup>1-4</sup> solutions of poly((*R*)-1-deuterio-*n*-hexyl isocyanate) (**1**,  $\alpha$ PdHIC) show extraordinarily large optical rotations (OR, negative) compared with its monomer in organic solvents. Recently, Green et al.<sup>5</sup> have found that poly((*R*)-2-deuterio-*n*-hexyl isocyanate) (**2**,  $\beta$ PdHIC), which has a chiral center on the  $\beta$ -carbon on the side chain, also exhibits substantially the same OR behavior, although to a less extent. This is a remarkable phenomenon on three accounts. First, it is an enormous amplification of a structural deuterium isotope effect, since the deuterated parent monomer shows only a very small optical rotation. Second, the optical rotation is highly temperature dependent, approaching its maximum value at a very low temperature. Third, the OR is remarkably molecular-weight dependent, being close to zero for oligomers and approaching its maximum value at very high degrees of polymerization for any given temperature. The molecular-weight dependence of OR of hexane, 1-chlorobutane, and dichloromethane (DCM) solutions of  $\beta$ PdHIC is the subject of the present study. These solvents were chosen because they allowed optical rotation measurements in the ultraviolet region and the stiffness of the polymer chain differs significantly in them.



Polyisocyanates,  $-(\text{CO}-\text{N}(\text{R}))_n-$ , are known to be stiff polymers<sup>6-12</sup> because of their backbone consisting of consecutive amide bonds, which forms a helical conformation.<sup>8,13-19</sup> This is due to steric hindrances preventing the amide bonds from staying coplanar, whether trans or cis. The helical sections tend to be very long, because reversal of the helical sense requires that at least one monomer unit obtains a reversal conformation and such a conformation is of relatively high energy. The helices may be either left-handed (*M*) or right-handed (*P*), and if a polyisocyanate has no chirotopic center on its side groups, the *M* and *P* helices are mirror images of each other and are therefore of equal probability. In such a situation no optical rotation will be observed. Goodman and Chen<sup>20,21</sup> synthesized for the first time optically active polyisocyanates soluble in organic solvents which showed large optical activity and proposed that a helical conformation would exist in the optically active polyisocyanates.

<sup>†</sup> Taken in part from the doctoral thesis of C. Andreola, Polytechnic University, 1991.

\* Abstract published in *Advance ACS Abstracts*, January 15, 1995.

In  $\beta$ PdHIC the mirror image symmetry is broken by the deuterated stereocenter. A very small energy difference exists between the deuterated monomer units in their *M* and *P* conformation. However, this small difference is greatly amplified by the length of the helical sequences. Thus long *M* and *P* helices may differ in energy by an amount commensurable with the thermal energy  $RT$  and consequently be unevenly distributed. This is the source of the observed  $OR^{1-5,22}$  and explains qualitatively the amplification of the small isotope effect as well as its dependence on temperature and molecular weight.

A quantitative theory of the specific rotation  $[\alpha]$  as a function of the absolute temperature  $T$  and degree of polymerization  $N$  was derived by a very simple statistical mechanical model.<sup>2</sup> The model assumes that each monomer unit can exist in either one of three microscopic states: helical left-handed (*M*), helical right-handed (*P*), or reversal from one helical sense to the other (*R*). The energy difference between the helical states,  $2\Delta E_h = E_M - E_P$ , is much smaller than the thermal energy  $RT$  at all temperatures of interest. While only energy differences count, a reference point of zero energy is usually chosen in statistical mechanical analyses. In our model it is the midpoint between *M* and *P*, which accordingly have the very small energies  $+\Delta E_h$  and  $-\Delta E_h$ , respectively. The energy of the reversal state,  $\Delta E_r$ , must be significantly larger than  $RT$ , or else the sense of the helical sequences would be reversed often and the sequences would be short, contrary to experimental observation.<sup>2,3</sup>

In our simple model the energies  $\Delta E_h$  and  $\Delta E_r$  were assumed to be constant, independent of temperature. Only the distribution among the states was assumed to be temperature dependent through their corresponding statistical weights (which are proportional to the probabilities of occurrence).

In a more realistic model, the energies attributed to the three states, *M*, *P*, and *R*, of the monomeric units should be recognized as free energies, being averaged over a large number of truly microscopic states that are assumed to belong to either of these states. They are, therefore, themselves functions of temperature. This more realistic model is adopted in the present study, where  $[\alpha]$  has been measured as functions of  $N$  as well as  $T$  over a very wide range of  $N$ . The assumed constant energies  $\Delta E_h$  and  $\Delta E_r$  are replaced by the corresponding free energies  $\Delta G_h(T)$  and  $\Delta G_r(T)$ . These free energies have been determined as functions of temperature by least-squares optimization that yields a best fit between calculated and observed  $[\alpha]$  over a wide range of  $N$  at each temperature. The enthalpies,  $\Delta H_h(T)$  and  $\Delta H_r(T)$ , and entropies,  $\Delta S_h(T)$  and  $\Delta S_r(T)$ , have been obtained from the temperature dependence of the free energies by the general thermodynamic relations. The free energy functions,  $\Delta G_h(T)$ , and hence  $\Delta H_h(T)$  and  $\Delta S_h(T)$ , refer to the differences between the *M* and *P* helix states.

The statistical mechanical derivation of the specific rotation  $[\alpha]$  as a function of  $T$  and  $N$  (eq 21 in ref 2) has not been affected at all by the new interpretation of the energies of the states *M*, *P*, and *R* as free energies. Only the statistical weights  $u_M$ ,  $u_P$ , and  $v$  are redefined as

$$\begin{aligned} u_M &= \exp[-\Delta G_h(T)/RT], & u_P &= \exp[+\Delta G_h(T)/RT] \\ v(T) &= \exp[-\Delta G_r(T)/RT] \end{aligned} \quad (1)$$

We present here  $[\alpha]$  as a function of  $T$  (through the

statistical weights) and of  $N$  in an approximate form (eq 23 in ref 2) that will facilitate the discussion of the results:

$$[\alpha]/[\alpha]_m = \frac{(\delta u/w) \frac{1 - a \exp(-2wN) - b[1 - \exp(-2wN)]/wN}{1 + a \exp(-2wN)}}{1 + a \exp(-2wN)} \quad (2)$$

where  $[\alpha]_m$  is the maximum value obtained by  $[\alpha]$  when all helices have only one sense, that of *P*. Here,  $\delta u$ ,  $w$ ,  $a$ , and  $b$  are functions of  $T$  only, which may be obtained from the two independent free energy functions  $\Delta G_h(T)$  and  $\Delta G_r(T)$  through the statistical weights of eq 1 as follows:

$$\begin{aligned} \delta u &= \frac{1}{2}(u_P - u_M), & w &= (\delta u^2 + v^2)^{1/2} \\ a &= (w - v)/(w + v), & b &= v/(w + v) \end{aligned} \quad (3)$$

The number of monomeric units in the reversal state *R* per molecule  $n_v$  is given by

$$\begin{aligned} n_v &= (Nv^2/w) \times \\ &\frac{1 + (w - v)/(wN) - [a + (w - v)/(wN)] \exp(-2wN)}{1 + a \exp(-2wN)} \end{aligned} \quad (4)$$

It can be shown that eq 2 is a very close approximation to eq 21 of ref 2 within the ranges of parameter values of interest and hardly introduces any errors in analyzed results. For  $wN > 2$ , the exponential terms in eq 2 may be neglected to a good approximation, and eq 2 is simplified to

$$[\alpha]/[\alpha]_m = (\delta u/w) \{1 - v/(w + v)wN\} \quad (5)$$

This equation shows that the number-average degree of polymerization  $N_n$  is appropriate for a polydisperse sample of sufficiently high molecular weight. The same  $N_n$  dependence is seen in the helix-coil transitions in polypeptides.<sup>23-25</sup> The behavior of eq 2 in different regions of  $wN$  will be discussed below in the light of the analysis of experimental  $[\alpha]$  as a function of  $N$ . The applicability of eq 2 to real systems can be confirmed by comparing it with experimental data for  $[\alpha]$  vs  $N$  at a fixed solvent condition, with  $[\alpha]_m$ ,  $\Delta G_h(T)$ , and  $\Delta G_r(T)$  being arbitrary functions of  $T$ .

Optical rotation measurement was performed on hexane, 1-chlorobutane, and dichloromethane (DCM) solutions of a number of narrow molecular weight distribution samples of  $\beta$ PdHIC ranging in weight-average degree of polymerization  $N_w$  between 41 and 5500, and the results were presented in terms of the specific rotation at 300 nm,  $[\alpha]_{300}$ . The  $[\alpha]_{300}$  observed changed remarkably with  $T$ ,  $N_w$ , and solvent. The  $[\alpha]_{300}$  data obtained have been analyzed to find that eq 2 is valid within the experimental uncertainties of  $[\alpha]_{300}$  and  $N_w$ , thus substantiating the validity of the theory. The analysis has shown that in hexane at 25 °C the free energy of the *P* state is lower than that of the *M* state only by 0.74 cal mol<sup>-1</sup>, whereas the *R* state has an energy excess as high as 3900 cal mol<sup>-1</sup>. Thus the helix sense is only rarely reversed on the same chain.

## Experimental Section

**Preparation of Fractionated Samples.** An original sample  $\beta$ 250 of about 2 500 000 molecular weight synthesized

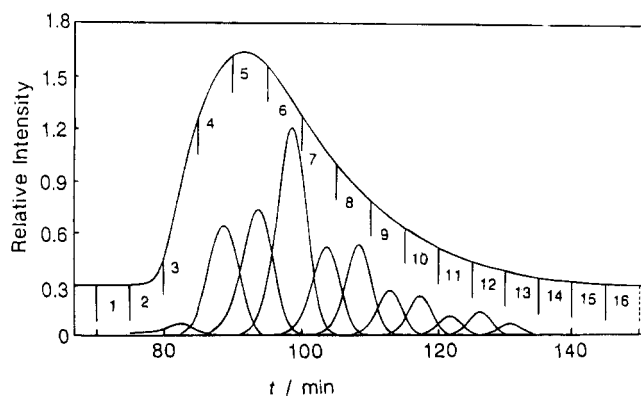


**Figure 1.** Gel permeation chromatograms of  $\beta 10$ -A and their fractions.

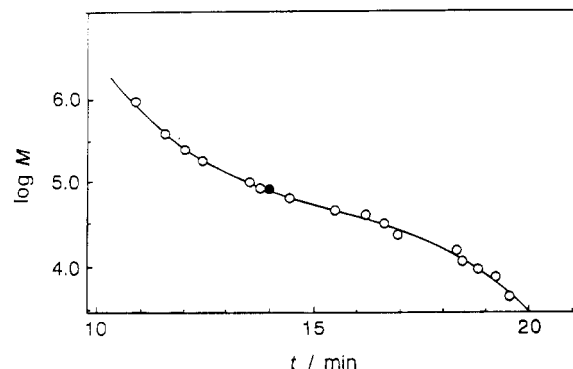
as described elsewhere<sup>5</sup> was degraded by adding trifluoroacetic acid in a chloroform solution. The reaction was allowed to proceed in a Ubbelohde viscometer, with the flow time being used to monitor the extent of degradation, and stopped finally with triethylamine. The resulting polymer was recovered by pouring the solution into a large excess of methanol. Two samples of about 100 000 molecular weight,  $\beta 10$ -A and  $\beta 10$ -B, and one sample of 200 000 molecular weight,  $\beta 20$ , were obtained in this way.  $\beta 10$ -A dissolved in chloroform was separated into many fractions on a gel permeation chromatograph equipped with a TSK G4000H8 column (21.5 mm in the inner diameter and 600 mm long) in six runs. In each run 1 cm<sup>3</sup> of the solution with the mass concentration  $2 \times 10^{-3}$  g cm<sup>-3</sup> was chromatographed, eluting at a flow rate of 1 cm<sup>3</sup>/min.

Figure 1 shows a chromatogram of one such solution of  $\beta 10$ -A, where vertical segments indicate how each fraction was separated and fractions A-3 through A-13 were selected for physical measurements. Sample  $\beta 10$ -B was separated similarly to obtain fractions B-3 through B-15. It was confirmed that each B-*i* fraction had essentially the same molecular weight as fraction A-*i*. Sample  $\beta 20$  was separated in 80 runs, 0.5 cm<sup>3</sup> for each run, to obtain 11 fractions C-3 through C-13, using TOSOH TSK G5000HxL and TSK G4000HxL columns connected in series. Each fraction was recovered by evaporating chloroform under reduced pressure and dried in vacuo for 2 days.

**Gel Permeation Chromatography.** Chromatograms were taken at 40 °C on a TOSOH HLC8020 analytical gel permeation chromatograph equipped with TOSOH columns TSK G5000HxL and TSK G4000HxL connected in series using chloroform as the eluent and with a UV detector operating at 254 nm.

**Optical Rotation Measurement.** Optical rotation measurements were made on a JASCO ORD/UV-5 using a quartz cell of 10 cm path length at wavelengths of light between 300 and 600 nm, with the results being expressed in terms of specific rotation  $[\alpha]_\lambda$  at wavelength  $\lambda$ . In actual analyses, only the specific rotation at 300 nm,  $[\alpha]_{300}$ , was used, which was expressed in units of 10<sup>-1</sup> deg cm<sup>-2</sup> g<sup>-1</sup>.

**Concentration Determination.** Commercial *n*-hexane, toluene, 1-chlorobutane, chloroform, and dichloromethane were purified according to the usual procedure. The purified chloroform with 0.3 wt % of ethanol added was used for optical rotation measurements. Amounts of fractionated samples were too small to be weighed directly so that no direct determination of their concentrations was attempted. Therefore the concentrations *c* of the solutions used for optical rotation measurements were evaluated from the optical density  $[\text{OD}]_{250}$  at 250 nm of the solution, using the relation  $[\text{OD}]_{250} = \gamma c$ , where  $\gamma$  is the extinction coefficient. It was found however that  $\gamma$  depends on the polymer molecular weight, which is empirically expressed by  $\gamma = \gamma_0(1 - B/M)$  irrespective of solvent;  $\gamma_0 = 3.08 \times 10^4$  cm<sup>3</sup> g<sup>-1</sup> and  $B = 2.50 \times 10^3$ . The correction term  $B/M$  became appreciable only below  $M = 20$  000.



**Figure 2.** GPC calibration curve for  $\beta$ PdHIC in chloroform constructed with reference poly(hexyl isocyanate) samples of known weight-average molecular weights  $M_w$ . Filled circle: data for sample A-5 (see text).

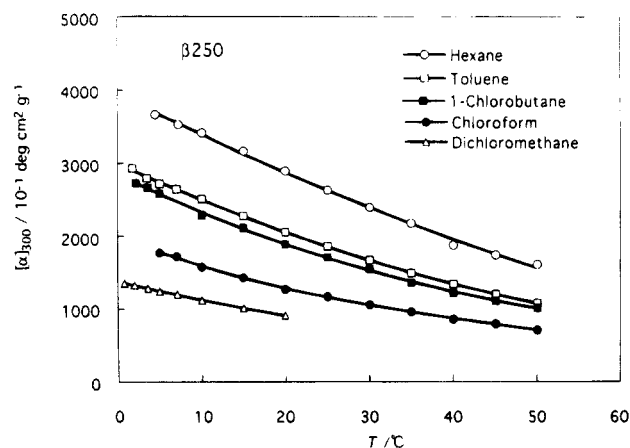


**Figure 3.** Specific rotation  $[\alpha]_{300}$  plotted against temperature for sample  $\beta 250$  in the indicated solvents.

## Results

**Molecular Weight Determination.** As will be shown elsewhere,<sup>26</sup>  $\beta$ PdHIC and PHIC have essentially the same dimensions in solution. Thus it is expected that the molecular weight–elution time calibration curve for the gel permeation chromatogram will be the same for the two polymers. On this premise, the calibration curve for chloroform solutions was constructed using a number of narrow-distribution PHIC samples of known weight-average molecular weights  $M_w$  from our stock as the reference materials. Figure 2 shows the result for the series connection of columns TSK G5000HxL and TSK G4000HxL with chloroform as the eluent; the solid curve represents the calibration curve, which was constructed so that they would reproduce the known  $M_w$  within 3%. A filled circle in the figure represents the data for a fractionated  $\beta$ PdHIC sample A-5, whose  $M_w$  was determined to be 82 000 by light scattering. This data point falls close on the calibration curve in accordance with the above premise.

The molecular weight distribution and number- and weight-average molecular weights  $M_n$  and  $M_w$  of each fraction were determined from the corresponding chromatogram using the calibration curve thus constructed. The weight-average degrees of polymerization  $N_w$  were calculated from  $M_w$  by  $N_w = M_w/128.2$ . Table 1 summarizes the values of  $N_w$  and the polydispersity index  $M_w/M_n$  thus determined for fractions A-3 through A-13, B-3 through B-15, and C-3 and through C-7. It can be seen from the values of  $M_w/M_n$  that the A and B series samples are nearly monodisperse and the C series samples are reasonably narrow as well. Therefore they

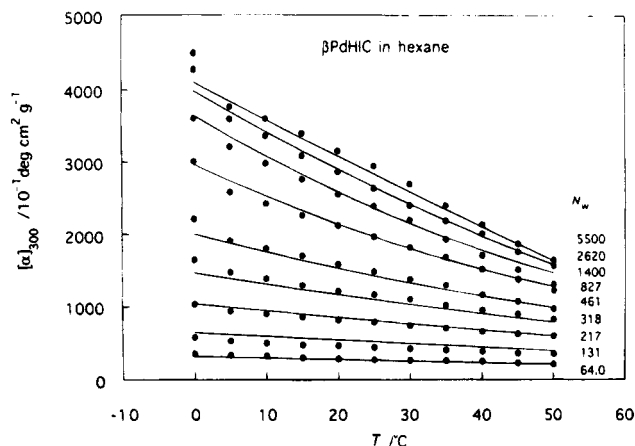


**Figure 4.** Plots of  $[\alpha]_{300}$  against temperature for  $\beta$ PdHIC fractions of different  $N_w$  in hexane at the indicated temperatures. Solid curves: theoretical values calculated by eq 2 (see text).

**Table 1.** Values of  $N_w$  and  $M_w/M_n$  for  $\beta$ -PdHIC Samples

sample	$N_w$	$M_w/M_n$
A-3	1360	1.07
A-4	847	1.04
A-5	631	1.03
A-6	486	1.02
A-7	390	1.01
A-8	320	1.01
A-9	265	1.01
A-10	216	1.01
A-11	172	1.02
A-12	130	1.03
A-13	92.8	1.03
B-3	1370	1.06
B-4	827	1.03
B-5	582	1.02
B-6	461	1.01
B-7	377	1.01
B-8	318	1.01
B-9	264	1.01
B-10	217	1.01
B-11	172	1.02
B-12	131	1.03
B-13	94.4	1.04
B-14	64	1.06
B-15	41	1.08
C-3	5500	1.19
C-4	3710	1.14
C-5	2620	1.12
C-6	1900	1.11
C-7	1400	1.11

are regarded as monodisperse and their  $N_w$  will be used for  $N$  in the theoretical treatment to follow and appear when necessary.

**Optical Rotation Data.** Figure 3 shows plots of  $[\alpha]_{300}$  vs temperature for sample  $\beta$ 250 in various solvents;  $[\alpha]_{300}$  is expressed in the conventional units of  $10^{-1} \text{ deg cm}^2 \text{ g}^{-1}$ . In either solvent  $[\alpha]_{300}$  decreases monotonously with increasing temperature but depends remarkably on solvent at fixed temperatures. It is noted that when compared with hexane (25 °C), toluene (10, 25, and 40 °C), 1-chlorobutane (25 °C), chloroform (25 °C), and dichloromethane (20 °C) solutions,  $[\alpha]_{300}$  increases with increasing intrinsic viscosity.<sup>26</sup>

Figure 4 shows the temperature dependence of  $[\alpha]_{300}$  for  $\beta$ PdHIC fractions of the indicated weight-average degree of polymerization  $N_w$  in hexane, where the solid curves represent theoretical values which will be explained later. For a high molecular weight sample,  $[\alpha]_{300}$  decreases steadily with increasing temperature but changes only slightly for low molecular weight

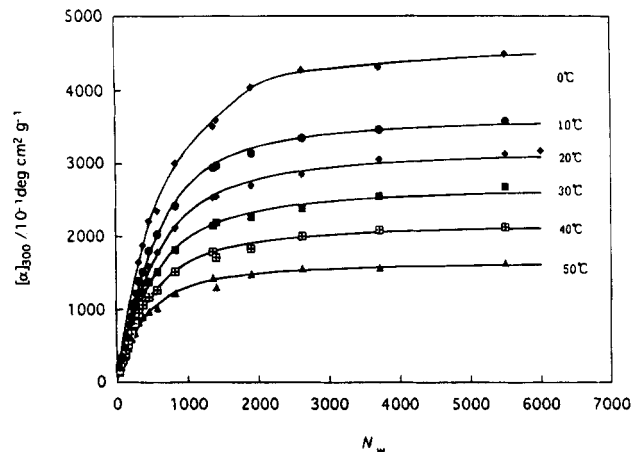


**Figure 5.** Dependence of  $[\alpha]_{300}$  on degree of polymerization  $N_w$  for fractions of  $\beta$ PdHIC in hexane at the indicated temperatures.

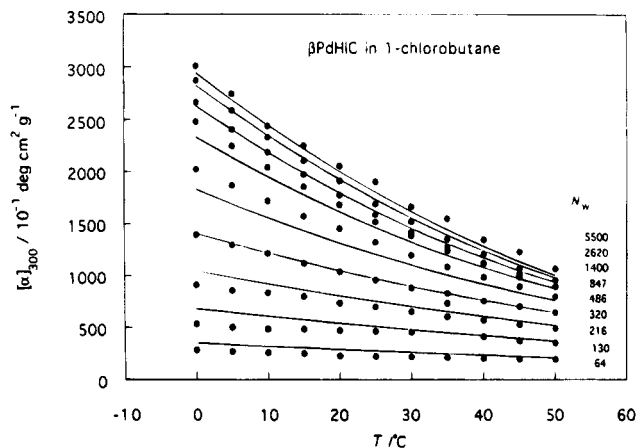


**Figure 6.** Plots of  $[\alpha]_{300}$  against temperature for  $\beta$ PdHIC fractions of different  $N_w$  in 1-chlorobutane. Solid curves: theoretical values calculated by eq 2 (see text).

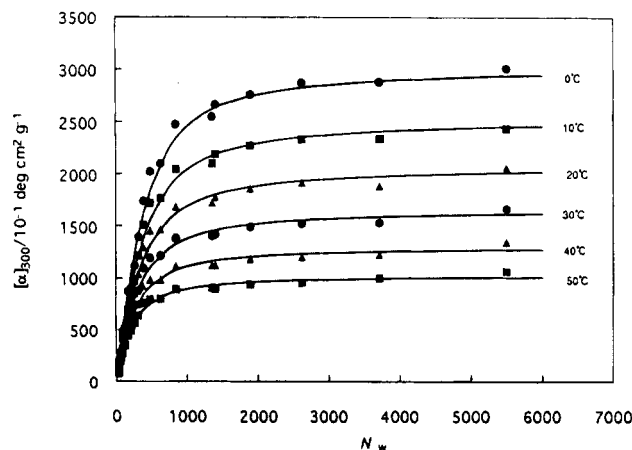


**Figure 7.** Dependence of  $[\alpha]_{300}$  on degree of polymerization  $N_w$  for fractions of  $\beta$ PdHIC in 1-chlorobutane at the indicated temperatures.

fractions. An upswing below 5 °C for very high  $N_w$  resembles a similar trend found by Green et al.<sup>27</sup> and may be related to gelation or aggregation as claimed by these authors. At a fixed temperature, it depends remarkably on  $N_w$ , which is shown more clearly in Figure 5. It is seen that  $[\alpha]_{300}$  increases rapidly with  $N_w$  below 1000 but tends to level off at a constant value at higher  $N_w$ . Figures 6–8 illustrate similar data for 1-chlorobutane and DCM solutions, where the temperature dependence is monotonous and the molecular-

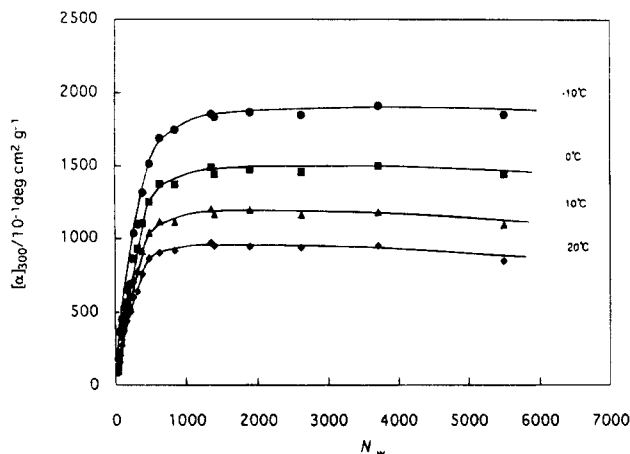


**Figure 8.** Dependence of  $[\alpha]_{300}$  on degree of polymerization  $N_w$  for fractions of  $\beta$ PdHIC in dichloromethane at the indicated temperatures.

weight dependence is similar to those for the hexane solutions. All these results are used to examine the validity of our previous analysis and establish the involved mechanism in more detail. These  $\beta$ PdHIC fractions are characterized by  $N_w/N_n$  smaller than 1.2, and thus in the analysis to follow, they are regarded as monodisperse, with the degree of polymerization  $N$  equated to their weight averages  $N_w$  unless specified.<sup>28</sup>

## Discussion

**How To Analyze the Experimental Data by Means of the Statistical Mechanical Theory.** Equation 2 shows that  $[\alpha]$  is a complicated but unique function of  $N$  with  $w$  and  $v$  (or  $\Delta G_h(T)$  and  $\Delta G_r(T)$ ) and with  $[\alpha]_m$  as the parameters under a specified solvent condition. When a number of  $[\alpha]$  vs  $N$  data points are available covering a wide range in  $N$ , they may be compared with eq 2 to test it with respect to molecular-weight dependence. If the theoretical dependence is confirmed, then the values of all three parameters may be determined by fitting the data to the theory.

**Test of the Theory and Determination of the Best Fit Parameters.** Data for  $[\alpha]$  vs  $N$  are analyzed in the following way. Let us define the residue  $\sigma$  for  $[\alpha]$  by

$$\sigma^2 = (1/n) \sum_{j=1}^n \{ \ln([\alpha]_{\text{meas}}/[\alpha]_{\text{calc}}) \}_j^2 \quad (6)$$

where  $n$  is the number of data sets of samples of different  $N$  and the superscripts "meas" and "calc" represent the measured and calculated  $[\alpha]$ , respectively. The accuracy of  $[\alpha]_{\text{meas}}$  was determined from those of the measured optical rotation and concentration. Both these measurements were equally accurate at all values encountered, resulting in an equal experimental uncertainty in the relative value of  $[\alpha]_{\text{meas}}$ . Thus it follows that the ratio  $[\alpha]_{\text{meas}}/[\alpha]_{\text{calc}}$  should be taken as the measure for the agreement between experiment and theory. Since there is no way of assessing the uncertainty of the  $N_w$  values obtained, they are regarded as accurate.<sup>28</sup> For a particular set of data at a given temperature  $T$ , first, trial-and-error procedures are repeated to sort the values of  $\Delta G_h(T)$  and  $\Delta G_r(T)$  minimizing  $\sigma$  for various values of  $[\alpha]_m$ . The best fit between experiment and theory may be achieved with the value of  $[\alpha]_m$ , which minimizes  $\sigma$ , and, in turn, the corresponding set of  $[\alpha]_m$ ,  $\Delta G_h(T)$ , and  $\Delta G_r(T)$  values

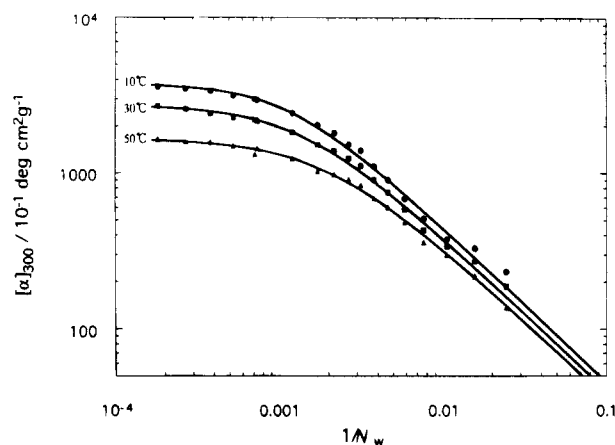


**Figure 9.** Test of eq 2 with the three adjustable parameters,  $\Delta G_h(T)$ ,  $\Delta G_r(T)$ , and  $[\alpha]_m$ . Solid curves: theoretical values with the values for  $2\Delta G_h(T)/RT$ ,  $\Delta G_r(T)/RT$ ,  $[\alpha]_m/(10^{-1} \text{ deg cm}^2 \text{ g}^{-1})$ , and  $\sigma$  of 0.00207, 7.15, 4770, and 0.019, respectively, at 10 °C, 0.00167, 6.65, 5120, and 0.011 at 30 °C, and 0.00196, 6.26, 3660, and 0.0035 at 50 °C.

may be taken to be optimal. Figure 9 illustrates the result from such an optimization with the data for the hexane solutions at 10, 30, and 50 °C, where the solid curves represent the theoretical values calculated by eq 2 with the optimal parameter values obtained. It is seen that the agreement between experiment and theory is excellent except at very low  $N_w$ , with the values of  $\sigma$  being 0.019–0.0035. Thus we conclude that eq 2 represents the correct molecular-weight dependence of optical rotation. However, it is difficult to accept the derived parameter values as correct, particularly the value of  $[\alpha]_m$ , varying remarkably with temperature. This is because it should be characteristic of the totally right-handed helical conformation of the backbone, which is expected to be specific to a particular solvent. It is also unnatural that  $\Delta G_h(T)$  does not show a monotonous change with temperature. Therefore we have abandoned this approach. The derived values for the parameters have no physical significance.

**Determination of  $[\alpha]_m$ .** The statistical mechanical theory introduced above contains two statistical mechanical parameters,  $\Delta G_h(T)$  and  $\Delta G_r(T)$ , and  $[\alpha]_m$ , which would be attained at sufficiently low temperatures. As seen in the data presented up to this point, no such limiting value is realized. Therefore we will determine  $[\alpha]_m$  in the following way using optical rotation data for poly(*(R)*-2,6-dimethylheptyl isocyanate) (PNIC). It has been shown that PNIC showed almost no temperature dependence of optical rotation and would be perfectly left-handed.<sup>29,30</sup> This inference is justified with optical rotation data shown in Figure 10, where the  $[\alpha]_{300}$  for PNIC  $[\alpha]_{300}^{\text{PNIC}}$  is plotted against temperature for various solvents. It can be seen that  $[\alpha]_{300}^{\text{PNIC}}$  stays almost constant within the temperature ranges examined, although it differs largely for different solvents. Therefore we here assume that the values for  $[\alpha]_m$  (corrected for the difference in monomer molecular weight and ignoring at 300 nm the reasonably very small relative contribution of the side chain stereocenter) may be the same for  $\beta$ PdHIC and PNIC on a given solvent condition. On this basis, the values of  $[\alpha]_m$  for  $\beta$ PdHIC are evaluated using the relation

$$[\alpha]_m = \frac{169}{128} |[\alpha]_{300}^{\text{PNIC}}| \quad (7)$$

where the coefficient 169/128 stands for the correction

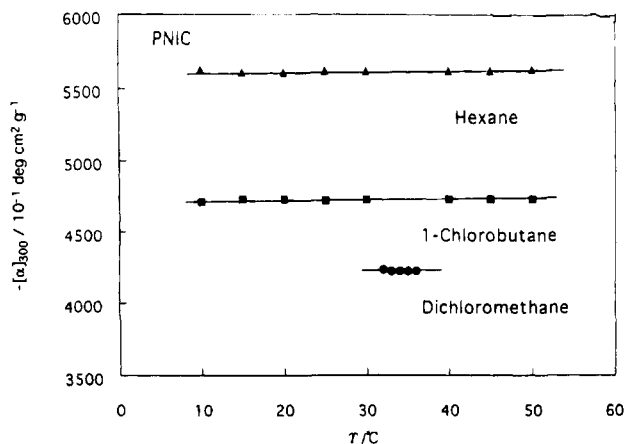


**Figure 10.** Plots of  $[\alpha]_{300}$  vs temperature for poly((R)-2,6-dimethylheptyl isocyanate) in various solvents.

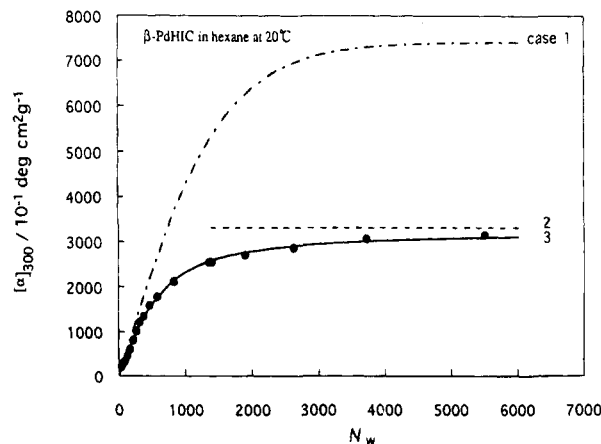


**Figure 11.** Test of theoretical predictions for three cases 1, 2, and 3 with small, large and medium values of  $N$ , respectively, with the data for the hexane solutions at 20 °C. Curves, theoretical values with the parameter values  $2\Delta G_h(T)/RT = 0.0013$ ,  $\Delta G_r(T)/RT = 6.65$ , and  $[\alpha]_m = 7420 \times (10^{-1} \text{ deg cm}^2 \text{ g}^{-1})$ .

factor for monomer molecular weight with the result  $[\alpha]_m = 7420, 6240$ , and  $5590 \text{ } 10^{-1} \text{ deg cm}^2 \text{ g}^{-1}$  for hexane, 1-chlorobutane, and DCM, respectively.

In the previous study,<sup>2</sup> three different cases were considered depending on the magnitude of  $N$ . The first case is defined for  $wN \ll 1$ , where the chain length is too short to accommodate even a single reversal point, and hence each chain is either a left-handed, or right-handed helix. On the other hand, case 2 is defined for  $wN \gg 1$  and  $[\alpha]$  does not depend on  $N$ . Case 3 is the general case valid for any value of  $wN$ , which is given by eq 2. Figure 11 examines this theoretical prediction with the hexane data at 20 °C. Here the solid curve represents the results of theoretical values for case 3, and the dashed curve represents the case 1 calculation. The latter is seen to be largely above the data points. It was impossible to find an appropriate  $\Delta G_h(T)$  value, which would reproduce these data points over the range of  $N$  examined. The case 2 values shown by the dash-dot curve cannot fit the experimental data at all  $N_w$ . We find from this comparison that only the general case 3 may be applied to the present data. Indeed, as will be shown below, the number  $n_v$  of helix reversal per molecule is predicted to be proportional to  $N$  and as large as 2 even for  $N$  of 500 at 20 °C. Thus we conclude that all these results substantiate the accuracy of eq 2 and thus validate the molecular mechanism described.

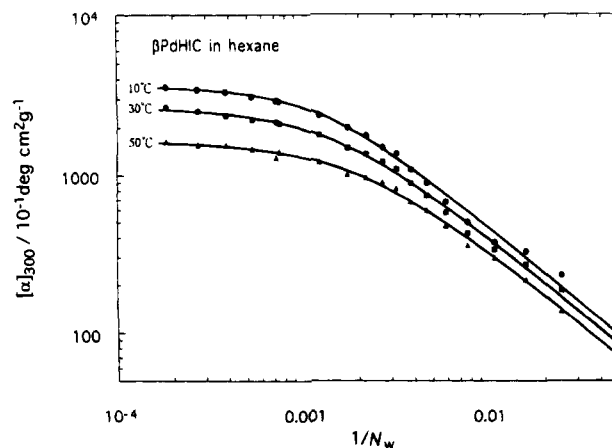


**Figure 12.** Fitting by eq 2 with data for hexane solutions at the indicated temperatures. Solid curves, theoretical values calculated by eq 2 with the parameter values given by eqs 8 and 9.

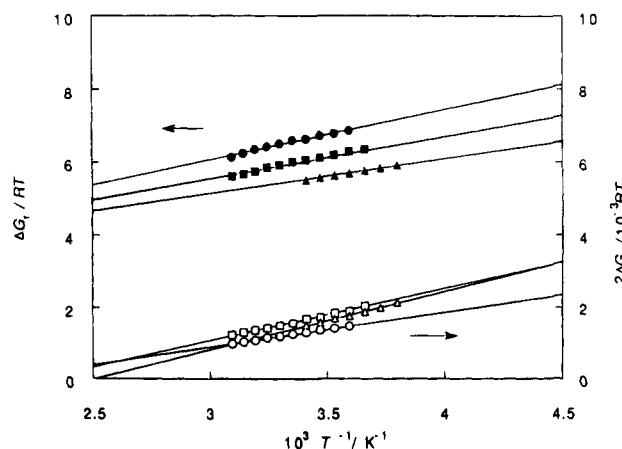


**Figure 13.** Plots of  $2\Delta G_h(T)/RT$  and  $\Delta G_r(T)/RT$  vs  $1/T$  for the three solvents investigated: (○,●) in hexane; (□,■) in 1-chlorobutane; (△,▲) in dichloromethane; straight lines, eqs 8–13.

If we assume that the theory is valid for the particular system of interest, we may use a nonlinear least-squares method based on  $\sigma^2$  to evaluate the optimal values of the parameters involved. In doing so, we have to assume  $\Delta H_h$ ,  $\Delta S_h$ ,  $\Delta H_r$ ,  $\Delta S_r$ , and  $[\alpha]_m$  to be independent of temperature within the temperature range concerned. However, this may be one of the conclusions to be reached from the analysis, and this method cannot be used to validate the theoretical equation and has not been used in the present analysis.

We have analyzed data as functions of  $N$  by eq 2 with the  $[\alpha]_m$  values estimated above. Figure 12 illustrates the results for the hexane solutions at the indicated temperatures, where the theoretical values (solid curves) fit the experimental data (symbols) accurately; indeed the value of  $\sigma$  is 0.021, 0.012, and 0.0036, respectively, at the three temperatures. Data at other temperatures and for 1-chlorobutane and DCM solutions were analyzed similarly. The average value of  $\sigma$  was 0.0085, 0.038, and 0.058 for hexane, 1-chlorobutane, and DCM, respectively. The fitting is not so precise for 1-chlorobutane and DCM as for hexane.

**Temperature Dependence of  $\Delta G_h(T)$  and  $\Delta G_r(T)$ .** Figure 13 shows plots of  $2\Delta G_h(T)/RT$  and  $\Delta G_r(T)/RT$  against  $1/T$  for hexane, 1-chlorobutane, and DCM solutions. The values of  $2\Delta G_h(T)/RT$  and  $\Delta G_r(T)/RT$  change significantly with  $1/T$  within the range of  $T$  investigated for either solvent and are represented reasonably ac-

**Table 2. Statistical Mechanical Parameters for the Hydrogen–Deuterium Isotope Effect and Helix Reversal for Poly(*R*)-2-deuterio-*n*-hexyl isocyanate) in dilute solution**

	solvent		
	hexane	1-chlorobutane	dichloromethane
$\Delta H_h/(\text{cal mol}^{-1})$	0.972	1.46	1.63
$\Delta S_h/(\text{cal mol}^{-1} \text{K}^{-1})$	0.00204	0.00332	0.00408
$T_h/\text{K}$	480	440	400
$\Delta H_r/(\text{cal mol}^{-1})$	2750	2300	1900
$\Delta S_r/(\text{cal mol}^{-1} \text{K}^{-1})$	-3.84	-4.11	-4.53
$[\alpha]_m/(10^{-1} \text{ deg cm}^2 \text{ g}^{-1})$	7420	6240	5590
For $N = 2000$ at $20^\circ \text{C}$			
$\Delta G_h/(\text{cal mol}^{-1})$	0.382	0.487	0.434
$u_P:u_M$	1.00066:0.99934	1.00084:0.99916	1.0007:0.9993
$n_P:n_M$	69:31	65:35	58:42
$\Delta G_r/(\text{cal mol}^{-1})$	3876	3505	3228
$n_v$	2.39	4.66	7.72

curately by linear relations. For the hexane solutions they read

$$2\Delta G_h(T)/RT = -0.00205 + 0.979/T \quad (8)$$

$$\Delta G_r(T)/RT = 1.93 + 1380/T \quad (9)$$

The values at  $0^\circ \text{C}$  have not been used in this analysis, because they deviate significantly above the straight lines, probably due to the aggregation.<sup>27</sup> The straight line for  $2\Delta G_h(T)/RT$  appears to intersect the abscissa at a point well removed from the origin. The values for  $\Delta G_r(T)/RT$  also obey a linear relation but their relative change within the temperature range studied is smaller than for  $2\Delta G_h(T)/RT$ .

The data for the 1-chlorobutane and DCM solutions have been analyzed similarly, with the results

$$2\Delta G_h(T)/RT = -0.00334 + 1.47/T \quad (10)$$

$$\Delta G_r(T)/RT = 2.07 + 1160/T \quad (11)$$

for 1-chlorobutane and

$$2\Delta G_h(T)/RT = -0.00411 + 1.64/T \quad (12)$$

$$\Delta G_r(T)/RT = 2.28 + 955/T \quad (13)$$

for DCM. The numerical values for these parameters are summarized in Table 2.

It was found that these equations were accurate enough to reproduce the observed temperature dependence of  $[\alpha]_{300}$ . Indeed, the solid curves in Figures 4 and 6 represent the theoretical values calculated by eq 2 with these parameter values along with the values of  $[\alpha]_m$  assumed above, which follow closely the data points. It must be noted however that the relative change in  $\Delta G_r(T)/RT$  in this narrow temperature range is too small to argue the significance of the sign of the constant term. Thus eqs 9, 11, and 13 are used here only for numerical representation of the data, and this sign is not taken literally to infer the molecular mechanism involved. It is also gratifying that the value for  $\Delta G_r$  in 1-chlorobutane is the same as that obtained in 2-chlorobutane in an entirely different experiment involving chiral solvation to cause the helix sense bias.<sup>31</sup>

**Hydrogen–Deuterium Isotope Effect.** It is possible to evaluate by the standard thermodynamic procedure the enthalpies,  $\Delta H_h(T)$  and  $\Delta H_r(T)$ , and entropies,  $\Delta S_h(T)$  and  $\Delta S_r(T)$ , from the temperature dependence of  $\Delta G_h(T)$  and  $\Delta G_r(T)$ , which are defined by

$$\Delta G_i = \Delta H_i - T\Delta S_i \quad (i = h, r) \quad (14)$$

$\Delta G_h(T)$  may be written in an alternate form:

$$\Delta G_h = \Delta H_h(1 - T/T_h) \quad (15)$$

with  $T_h = \Delta H_h/\Delta S_h$ . This evaluation has been done using the data expressed by eqs 8–13, with the results shown in Table 2. This table also contains some average quantities of  $\beta\text{PdHIC}$  of  $N = 2000$  calculated with these parameters. The following features are noted in Table 2.

(1) The value of  $\Delta G_h(T)$  in hexane is very small at  $20^\circ \text{C}$  but changes significantly with temperature. Indeed, the enthalpic and entropic contributions to  $\Delta G_h(T)$ ,  $\Delta H_h$  and  $T\Delta S_h$ , are comparable at this temperature. The linearity of the plot of  $2\Delta G_h(T)/RT$  vs  $1/T$  in Figure 13 allows  $T_h$  to be determined with certainty, which is located around 480 K. Physically,  $T_h$  may be regarded as the critical temperature, above which the sign of  $[\alpha]_{300}$  would be inverted from positive to negative. This conversion could occur because the energetic contribution to  $\Delta G_h(T)$ , which favors the right-handed helix (*P*) at room temperature, is offset by the entropic contribution at higher temperature. Indeed quite a small value of 0.08 was obtained for  $[\alpha]_{300}/[\alpha]_m$  in toluene at  $90^\circ \text{C}$ .<sup>32</sup> It should be noted however that such a conversion may not be actually observed because of the degradation of the polymer at such high temperatures.

(2) The value of about 3.5 kcal mol<sup>-1</sup> for  $\Delta G_r(T)$  is close to our previous estimate,<sup>2,3</sup> and overwhelmingly enthalpic, which confirms the previous assertion. Thus we see that our previous analyses<sup>2,3</sup> were qualitatively correct and had provided the basic molecular mechanism of this isotope effect, although not accurate in quantitative terms. This arose because of the unfortunate situation that no detailed data for the  $N$  dependence of  $[\alpha]$  was available at the time of the analyses.

Conclusions 1 and 2 may be stated alternatively, that is, the *P* (right-handed) helix dwells in a slightly deep but narrow potential well in the conformational space compared with the *M* helix, whereas the helix reversal is highly unfavorable for energetic reasons.

(3) For  $\beta\text{PdHIC}$  in hexane at  $20^\circ \text{C}$ , the *P* helix is favored over the *M* helix only by 0.132% on the monomeric unit basis but the relative abundance of the *P* helix on the polymer chain of 2000 units is amplified to 69:31 by the cooperativity. This chain contains 2.42 helix reversal units; in other words, the helix reversal occurs only once in 826 monomeric units.

(4) The difference between different solvents resides in both  $\Delta G_h(T)$  and  $\Delta G_r(T)$ . However, the magnitude of  $[\alpha]_{300}$  for larger  $N_w$  is determined by the latter.



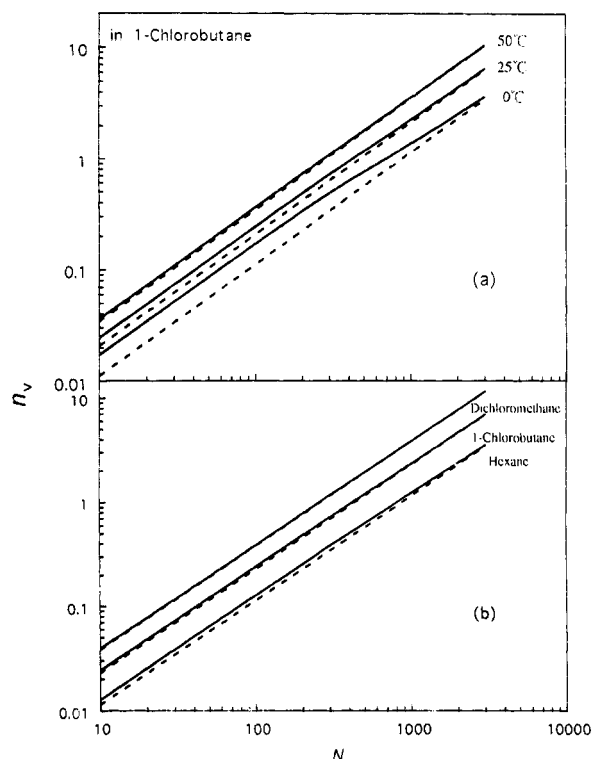


**Figure 14.** Number of helix breaks as a function of degree of polymerization: panel a, temperature dependence; panel b, solvent dependence. Solid curve, exact values; dashed lines, the asymptotic values, both calculated with the parameter values given in Table 2 (see text).

**Helix Reversal and Average Conformation.** It is well-known that the stiffness of polyisocyanates depends on such factors as the structure of the side chain, temperature, and solvent,<sup>6-12</sup> which has been attributed to their helical conformations.<sup>8,13-19</sup> Therefore it is interesting to ask how the thermodynamic parameters  $\Delta G_h(T)$  and  $\Delta G_r(T)$  are related to the chain stiffness expressed, for example, in terms of the persistence length  $q$ . In Figure 14 the number of helix reversal  $n_v$  under various solvent conditions is plotted double-logarithmically against  $N$ , calculated by eq 4 with the parameter values given in Table 2. It can be seen that  $n_v$  increases nearly linearly with increasing  $N$ ; the dashed lines of slope 1 represent the asymptotic values at high molecular weights expressed by  $n_v = Nv^2/w$ , and the deviation from this linearity becomes appreciable at low temperatures. For a particular solvent,  $n$  increases with increasing temperature, whereas at a fixed temperature it depends appreciably on solvent; at 20 °C  $n_v$  for  $N = 2000$  increases from 2.4 to 7.7 on going from hexane to DCM. This result indicates that a  $\beta$ PdHIC chain of this length contains a significant number of helix reversal points varying with solvent condition. It is noted that this change parallels the change in stiffness with solvent condition.<sup>26</sup>

If the helix reversal points would act as kinks, the chain should be regarded as a broken rod. Indeed a force-field calculation by Lifson et al.<sup>30</sup> shows that a reversal point may be regarded as a kink, where encompassing helical chains join at an angle of ca. 60°. Thus their directional continuity is interrupted, although the joint portion actually spreads over several monomeric units. This appears to be in contradiction with the well-established wormlike chain nature of polyisocyanates.<sup>6-12</sup> However, we do not consider the helix reversal would favor a discrete broken rod model

for polyisocyanate chains, because the helix reversal is a statistical event and occurs statistically over the entire chain. This reduces the discrete broken rod nature even if the reversal points are regarded as kinks. The correlation between optical activity and stiffness noted in the Results section should be explained consistently within the concept of the helix reversal. We are tempted to consider that the stiffness is also related to  $\Delta G_h(T)$ , which is connected with the intrinsic rigidity of the helical conformation as discussed by Cook et al.<sup>18</sup> However, we defer to draw a definite conclusion about this point until additional information becomes available about this and other polyisocyanates in various solvents. There is a report suggesting that the role of helix reversal appears to vary with polymers.<sup>33</sup> This problem will be pursued in a forthcoming investigation.<sup>26</sup>

As reported earlier,<sup>1-4</sup> poly(*R*)-1-deuterio-*n*-hexyl isocyanate ( $\alpha$ PdHIC, 1) also shows extraordinarily large optical rotations. In this polymer, deuterium is substituted on the  $\alpha$  carbon, one carbon-carbon bond closer to the main chain compared with  $\beta$ PdHIC. Thus the hydrogen-deuterium isotope effect may be more remarkable for this polymer than for  $\beta$ PdHIC. A detailed investigation of optical rotation of  $\alpha$ PdHIC will be reported in a following communication.<sup>32</sup> The original data for  $[\alpha]_{300}$  and the thermodynamic parameters have been compiled in a supplemental document and are available upon request to A.T.

**Acknowledgment.** The work at Osaka University was supported in part by a Grant-in-Aid for Scientific Research (No. 05044096) from the Ministry of Education, Science, and Culture of Japan. Thanks are due to Professor Takashi Norisuye for valuable discussions on the conformations of polyisocyanates. The work at the Polytechnic University was supported by the Chemistry and Materials Divisions of the National Science Foundation and by the Petroleum Research Fund, administered by the American Chemical Society.

## References and Notes

- (1) Green, M. M.; Andreola, C.; Munoz, B.; Reidy, M. P.; Zero, K. *J. Am. Chem. Soc.* **1988**, *110*, 4063.
- (2) Lifson, S.; Andreola, C.; Peterson, N. C.; Green, M. M. *J. Am. Chem. Soc.* **1989**, *111*, 8850.
- (3) Green, M. M.; Lifson, S.; Teramoto, A. *Chirality* **1991**, *3*, 285.
- (4) Andreola, C. Doctoral Thesis, Polytechnic University, 1991.
- (5) Unpublished work at the Polytechnic University. See also ref 4.
- (6) Berger, M. N.; Tidswell, B. M. *J. Polym. Sci., Polym. Symp.* **1973**, *42*, 1063.
- (7) Bur, A. J.; Fetters, L. J. *Chem. Rev.* **1976**, *76*, 727.
- (8) Rubingh, D. N.; Yu, H. *Macromolecules* **1976**, *9*, 681.
- (9) Murakami, H.; Norisuye, T.; Fujita, H. *Macromolecules* **1980**, *13*, 345.
- (10) Kuwata, M.; Murakami, H.; Norisuye, T.; Fujita, H. *Macromolecules* **1984**, *17*, 2731.
- (11) Itou, T.; Chikiri, H.; Teramoto, A.; Aharoni, S. M. *Polym. J.* **1988**, *20*, 143.
- (12) Takada, S.; Itou, T.; Chikiri, H.; Einaga, Y.; Teramoto, A. *Macromolecules* **1989**, *22*, 973.
- (13) Shmueli, U.; Traub, W.; Rosenheck, K. *J. Polym. Sci., Part A-2* **1969**, *7*, 515.
- (14) Troxell, T. C.; Scheraga, H. A. *Macromolecules* **1971**, *4*, 528.
- (15) Han, C. C.; Yu, H. *Polym. Prepr. (Am. Chem. Soc., Div. Polym. Chem.)* **1973**, *14*, 121.
- (16) Tonelli, A. E. *Macromolecules* **1974**, *7*, 854.
- (17) Mansfield, M. L. *Macromolecules* **1986**, *19*, 854.
- (18) Cook, R. *Macromolecules* **1987**, *20*, 1961.
- (19) Cook, R. C.; Johnson, R. D.; Wade, C. G.; Munoz, B.; Green, M. M. *Macromolecules* **1990**, *23*, 3454.
- (20) Goodman, M.; Chen, S.-c. *Macromolecules* **1970**, *3*, 398.
- (21) Goodman, M.; Chen, S.-c. *Macromolecules* **1971**, *4*, 625.



- (22) Green, M. M.; Reidy, M. P.; Johnson, R. D.; Darling, G.; O'Leary, D. J.; Wilson, G. *J. Am. Chem. Soc.* **1989**, *111*, 6452.
- (23) Lifson, S.; Roig, A. *J. Chem. Phys.* **1961**, *34*, 1963.
- (24) Teramoto, A.; Fujita, H. *Adv. Polym. Sci.* **1975**, *18*, 65.
- (25) Teramoto, A.; Fujita, H. *J. Macromol. Sci., Rev. Macromol. Chem.* **1976**, *C15*, 165.
- (26) Gu, H.; Mukaida, F.; Nakamura, Y.; Teramoto, A.; Green, M. M. To be submitted to *Macromolecules*.
- (27) Green, M. M.; Khatri, C. A.; Reidy, M. P.; Levon, K. *Macromolecules* **1993**, *26*, 4723.
- (28) The  $N_w$  values of the C-series samples are not accurate because the series combination of columns TSK G5000HxL and TSK G4000 may not have the desired resolution for these samples. However, this is not serious for theoretical analysis because  $[\alpha]_{300}$  would not depend significantly at such high molecular weights. We have used  $N_w$  for  $N$  instead of  $N_n$ , which would be an appropriate average according to eq 5. However, this gives rise to no significant difference in the results of the analysis, particularly with samples C-3 through C-7, whose molecular weights are so high that  $[\alpha]_{300}$  depends only slightly on molecular weight; thus use of either  $N_n$  or  $N_w$  makes no difference in the theoretical analysis. ( $[\alpha]_{300}^{\text{meas}} - [\alpha]_{300}^{\text{calc}})^2$  has not been used as a criterion for the optimization, since the experimental uncertainty in  $[\alpha]_{300}$  resides in its relative value, not the absolute value, which is almost equal irrespective of the magnitude of  $[\alpha]_{300}$  (see text).
- (29) Sato, T.; Sato, Y.; Umemura, Y.; Teramoto, A.; Nagamura, Y.; Wagner, J.; Weng, D.; Okamoto, Y.; Hatada, K.; Green, M. M. *Macromolecules* **1993**, *26*, 4551.
- (30) Lifson, S.; Felder, C. E.; Green, M. M. *Macromolecules* **1992**, *25*, 4142.
- (31) Green, M. M.; Khatri, C.; Peterson, N. C. *J. Am. Chem. Soc.* **1993**, *115*, 4941.
- (32) Okamoto, N.; Mukaida, F.; Gu, H.; Sato, T.; Nakamura, Y.; Teramoto, A.; Green, M. M.; Andreola, C.; Peterson, N. C.; Lifson, S. Submitted to *Macromolecules*.
- (33) Green, M. M.; Gross, R. A.; Cook, R.; Schilling, F. C. *Macromolecules* **1987**, *20*, 2636.

MA941140U